

# Crystal Structures of the Vitamin D Nuclear Receptor Liganded with the Vitamin D Side Chain Analogues Calcipotriol and Seocalcitol, Receptor Agonists of Clinical Importance. Insights into a Structural Basis for the Switching of Calcipotriol to a Receptor Antagonist by Further Side Chain Modification

Giuseppe Tocchini-Valentini,<sup>S,†</sup> Natacha Rochel,<sup>S</sup> Jean-Marie Wurtz, and Dino Moras\*

Département de Biologie et de Génomique Structurales, IGBMC, CNRS/INSERM/Université Louis Pasteur, Parc d'Innovation BP10142, 67404 Illkirch Cedex, France

Received October 7, 2003

The plethora of actions of  $1\alpha,25(\text{OH})_2\text{D}_3$  in various systems suggested wide clinical applications of vitamin D nuclear receptor (VDR) ligands in treatments of inflammation, dermatological indication, osteoporosis, cancers, and autoimmune diseases. More than 3000 vitamin D analogues have been synthesized in order to reduce the calcemic side effects while maintaining the transactivation potency of these ligands. Here, we report the crystal structures of VDR ligand binding domain bound to two vitamin D agonists of therapeutical interest, calcipotriol and seocalcitol, which are characterized by their side chain modifications. These structures show the conservation of the VDR structure and the adaptation of the side chain anchored by hydroxyl moieties. The structure of VDR-calcipotriol helps us to understand the structural basis for the switching of calcipotriol to a receptor antagonist by further side chain modification. The VDR-seocalcitol structure, in comparison with the structure of VDR-KH1060, a superagonist ligand closely related to seocalcitol, shows adaptation of the D ring and position of C-21 in order to adapt its more rigid side chain.

## Introduction

Vitamin D is an important regulator of bone development and metabolism and calcium homeostasis. It also plays an important role in the regulation of cell growth and differentiation in cells.<sup>1,2</sup> The plethora of actions of  $1\alpha,25(\text{OH})_2\text{D}_3$  in various systems suggested wide clinical applications of VDR ligands in treatments of inflammation (rheumatoid arthritis, psoriatic arthritis), dermatological indication (psoriasis, photoaging), osteoporosis, cancers (breast, prostate, colon, leukemia), and autoimmune diseases (multiple sclerosis, type I diabetes). However, therapy using vitamin D is associated with hypercalcemic effects and soft tissue calcification. More than 3000 analogues have been synthesized in order to reduce the calcemic side effects while maintaining the transactivation potency of these ligands.<sup>3</sup> Some of these analogues have been clinically tested. In particular, calcipotriol<sup>4</sup> (MC903, Dovonex, Leo Pharmaceuticals, Denmark) has become a first-line drug for the topical treatment of psoriasis.<sup>5</sup> Calcipotriol has very limited calcemic side effects mainly because of its decreased affinity to DBP,<sup>6</sup> and it is more rapidly metabolized than the natural hormone.<sup>7</sup> Another interesting analogue, seocalcitol<sup>8</sup> (EB1089, Leo Pharmaceuticals, Denmark), is very potent on inhibiting cell

proliferation<sup>9</sup> and is currently being clinically tested systemically in cancer treatment.<sup>10</sup> This ligand presents a modified side chain that renders it less susceptible to catabolic degradation. By use of seocalcitol at doses that produce nonsignificant hypercalcemia, it is efficient in reducing tumor growth in *in vivo* studies of prostrate and breast carcinomas.<sup>8,9</sup>

The response to the hormone is triggered by its nuclear receptor, the vitamin D receptor (VDR), a member of the nuclear hormone receptor superfamily.<sup>11</sup> The binding of the ligand to the receptor induces a conformational change of the ligand binding domain (LBD) with consequent dissociation of corepressors and association with coactivators of the p160 family (SRC1),<sup>12</sup> cointegrators (CBP)<sup>13</sup> that remodel chromatin and mediator complexes (DRIP/TRAP)<sup>14</sup> that recruit RNA polymerase. Previously we have reported the crystal structures of hVDR LBD bound to  $1\alpha,25(\text{OH})_2\text{D}_3$  and to two 20-epi analogues.<sup>15,16</sup> These structures show an identical protein conformation with an adaptation of the ligands to the binding pocket. Different conformations are observed only for the  $17\beta$ -aliphatic chains that adapt their conformation to anchor the 25-hydroxyl group to the same residues, His305 and His397. Here, we describe the crystal structures of hVDR in complexes with two vitamin D analogues, calcipotriol and seocalcitol (Figure 1). One analogue presents a side chain resembling the side chain of the superagonist KH1060.<sup>16</sup> The other one presents a different skeleton, which is the template of new antagonists molecules.<sup>17</sup> Besides the therapeutical interest, the paper helps to clarify the functional behavior of these molecules.

\* To whom correspondence should be addressed. Phone: (33) 3 88 65 33 51. Fax: (33) 3 88 65 32 76. E-mail: moras@igbmc.u-strasbg.fr.

<sup>S</sup> These authors contributed equally to this work.

<sup>†</sup> Present address: Istituto di Genetica Molecolare, Consiglio Nazionale delle Ricerche, Via Abbiategrasso 207, I-27100 Pavia, Italy, and Istituto di Biologia Cellulare, Consiglio Nazionale delle Ricerche, Campus A, Buzzati-Traverso, Via Ramarini, 32, 00016 Monterotondo Scalo, Rome, Italy.

Ligand	Formula R =	Binding to hVDR $\Delta$	EC <sub>50</sub> (nM) <sup>21</sup>
1 $\alpha$ ,25(OH) <sub>2</sub> D <sub>3</sub>		100	0.18
calcipotriol		90	
seocalcitol		80	
KH1060		90	
ZK159222		-	0.4
Partial antagonist			
ZK168281		-	0.35
Antagonist			

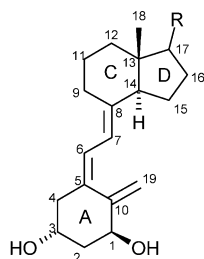


**Figure 1.** Vitamin D analogues discussed in this paper. Calcipotriol and seocalcitol correspond to the new crystal structures presented in this paper. 1 $\alpha$ ,25(OH)<sub>2</sub>D<sub>3</sub> is the natural ligand. KH1060 is a superagonist whose structure is closely related to that of seocalcitol. The crystal structure of the complex VDR-KH1060 is known.<sup>16</sup> ZK159222 and ZK168281 are partial or full antagonists whose side chain are based on the calcipotriol skeleton.

## Results and Discussion

**Structure Determination and Overall Description.** The synthetic analogues calcipotriol<sup>4</sup> and seocalcitol<sup>7</sup> (Figure 1) behave as full agonists of VDR. Both molecules show similar binding affinity as 1 $\alpha$ ,25(OH)<sub>2</sub>D<sub>3</sub> for the hVDR, high transactivation potency, and a similar profile of proteolysis as the natural ligand.<sup>18</sup> To obtain crystals of the hVDR LBD complexes, we used a hVDR LBD mutant lacking 50 residues in the loop connecting helices H1 and H3.<sup>15,16</sup> The same construct was previously used to solve the structure of the hVDR LBD bound to 1 $\alpha$ ,25(OH)<sub>2</sub>D<sub>3</sub><sup>15</sup> and to the 20-epi analogues,<sup>16</sup> 20-epi-1 $\alpha$ ,25(OH)<sub>2</sub>D<sub>3</sub> and KH1060. This mutant has the same biological properties (binding, transactivation in several cell lines, heterodimerization) as the hVDR LBD wild type.<sup>19</sup> The crystals were obtained under similar conditions and were isomorphous. The structures of VDR-calcipotriol and VDR-seocalcitol have been refined at resolutions of 2.1 and 2.5 Å, respectively. The experimental data and refinement statistics are summarized in Table 1. After refinement of the protein alone, the map shows an unambiguous electron density of where to fit the ligand. Parts A and B of Figure 2

**Table 1.** Data Collection and Refinement Statistics:

	ligand complexes	
	calcipotriol	seocalcitol
X-ray source	BM14	BM30
wavelength (Å)	0.918	1.00094
cell (Å) ( $\alpha = \beta = \gamma = 90^\circ$ )	$a = 45.248$ ; $b = 52.55$ ; $c = 132.909$	$a = 45.134$ ; $b = 52.528$ ; $c = 132.648$
space group	$P2_12_12_1$	$P2_12_12_1$
resolution (Å)	20.0–2.1	15.0–2.5
(last shell)	(2.15–2.10)	(2.59–2.50)
unique reflections	18 424	11 560
redundancy	3.8	4.0
completeness (last shell) (%)	98.2 (97.2)	98.3 (98)
$R_{\text{sym}}$ (last shell) (%)	7.3 (27.8)	7.1 (16.6)
$I/\sigma(I)$ (last shell)	16.5 (4.3)	15.1 (8.0)
$R_{\text{cryst}}$ (%)	17.9	17.0
$R_{\text{free}}$ (%)	21.4	20.3
rmsd bond length (Å)	0.0048	0.0056
rmsd bond angles (deg)	1.05	1.07
no. of non-hydrogen protein atoms	2013	2013
no. of non-hydrogen ligand atoms	30	33
no. of water molecules	184	83
$B_{\text{av}}$ , protein atoms (Å <sup>2</sup> )	21.8	23.0
$B_{\text{av}}$ , ligand atoms (Å <sup>2</sup> )	13.7	17.8
$B_{\text{av}}$ , water molecules (Å <sup>2</sup> )	36.7	35.4

show the ligand-omit maps calculated at the end of the refinement.

The hVDR LBD complexes adopt the canonical conformation of all previously reported agonist-bound nuclear receptor LBD with 12–13  $\alpha$ -helices organized in a 3-layered sandwich. In all the structures of hVDR bound to agonist ligands, a single conformation of the complex is observed. The position and conformation of the activation helix H12 is strictly maintained. The ligands adopt the same orientation in the pocket (Figure 2C). An adaptation of their conformation is observed in order to maintain the hydrogen bonds forming the anchoring points. When compared to the structure of hVDR-1 $\alpha$ ,25(OH)<sub>2</sub>D<sub>3</sub> complex, the atomic models of hVDR bound to calcipotriol and seocalcitol show rms deviations of 0.12 and 0.13 Å, respectively, on all atoms. The ligands are buried in the predominantly hydrophobic pocket that is conserved in all complexes. The sizes of the ligands are 381, 379, and 415 Å<sup>3</sup> for 1 $\alpha$ ,25(OH)<sub>2</sub>D<sub>3</sub>, calcipotriol, and seocalcitol, respectively. The volume of the ligand binding cavity is 660 Å<sup>3</sup>, and the ligand occupies 57%, 57%, and 61% of the pocket for 1 $\alpha$ ,25(OH)<sub>2</sub>D<sub>3</sub>, calcipotriol, and seocalcitol, respectively.

**Ligand Binding.** The interactions between the ligands and the receptor involve hydrophobic contacts and electrostatic interactions. The same interactions are observed between the protein and the A, secoB, and C/D rings, which present similar conformations (Figure 2C). Similarities extend to the water molecules that form a channel from position C2 of the A ring to the surface of the protein. As a consequence of its longer chain, the D ring of seocalcitol shifts by 0.4 Å, which results in a displacement of 0.7 Å for C21 compared to 1 $\alpha$ ,25(OH)<sub>2</sub>D<sub>3</sub>. The specific interactions observed in these complexes involve contacts with the aliphatic side chains (Table 2). The varying chain length of these ligands provides two examples of ligand adaptability between two anchoring points, 1-OH and 25-OH. The distance between the 1-hydroxy and the 25-hydroxy groups vary from 12.3 Å for calcipotriol, 12.7 Å for seocalcitol, and 13.0 Å for 1 $\alpha$ ,25(OH)<sub>2</sub>D<sub>3</sub> complex. These

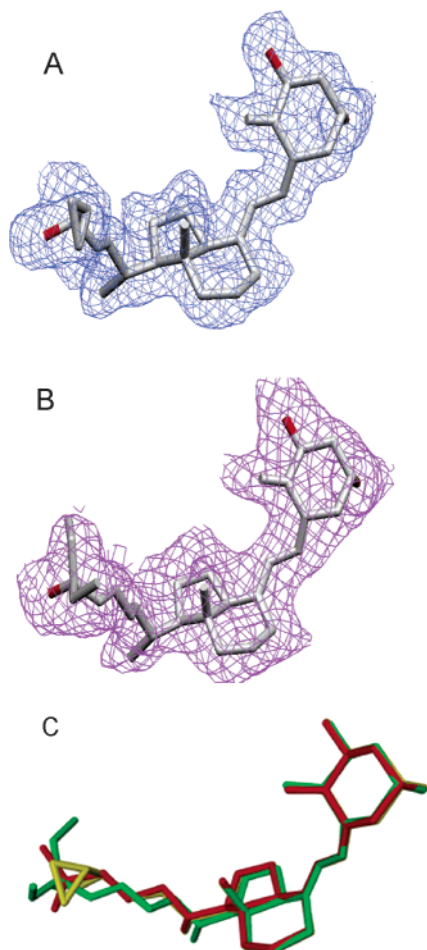


**Figure 2.** Conformations of the bound ligands. The ligands calcipotriol (A) and seocalcitol (B) are shown in their  $F_o - F_c$  electron density omit maps contoured at  $1.0\sigma$ . The ligands are shown in stick representation with carbon and oxygen atoms in gray and red, respectively. (C) Comparison of the ligand conformations of  $1\alpha,25(\text{OH})_2\text{D}_3$  (red), calcipotriol (yellow), and seocalcitol (green) in their VDR ligand binding pockets.

differences underlined the small degree of freedom allowed by these anchoring points.

In the VDR-calcipotriol structure (Figure 3A), despite the shorter side chain, a shift of 0.4 Å of His305 is sufficient to maintain the hydrogen bond with the hydroxyl group. A remarkable feature of calcipotriol compared to the natural ligand is the absence of direct contact with H12. Note that the absence of these direct contacts does not affect the transactivation potency of this ligand. Additional interaction observed concerns atoms of the cyclopropyl group and residues of H3. The cyclopropyl is oriented toward helix H3 and forms van der Waals contact with Leu227 (CD1 at 3.5 Å). The dihedral angle around the bond of the C24–C25 carbon atoms is *gauche minus* ( $-67^\circ$ ). In this orientation the ring is away from the activation helix H12. The closest residue is Val418 at 4.5 Å. The only stabilized interaction formed by the cyclopropyl is with the CA atom of Ala231 in H3. In this position a significant volume of the pocket is left unoccupied compared to seocalcitol, KH1060, and even  $1\alpha,25(\text{OH})_2\text{D}_3$ . Other rotamers around C24–C25 would not improve the situation.

In the VDR-seocalcitol structure (Figure 4A), all the residues forming the binding pocket adopt the same conformation as in the VDR- $1\alpha,25(\text{OH})_2\text{D}_3$  structure.

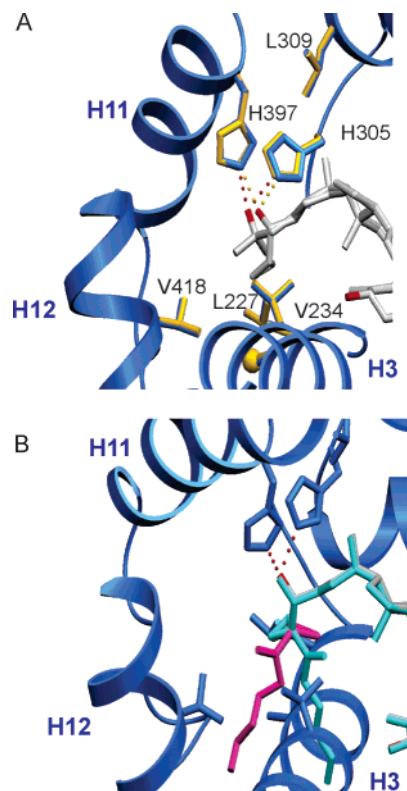


**Figure 3.** VDR-calcipotriol. (A) Superposition of the VDR-calcipotriol (blue) and VDR- $1\alpha,25(\text{OH})_2\text{D}_3$  (yellow) complexes. The view is restricted to the region of the protein (H3, H6, H11, and H12) contacting the aliphatic side chain. Only residues closer than 4.0 Å are shown. The ligands  $1\alpha,25(\text{OH})_2\text{D}_3$  and calcipotriol are shown in stick representation with carbon and oxygen atoms in gray and red, respectively. The hydrogen bonds formed by the 25-OH group of  $1\alpha,25(\text{OH})_2\text{D}_3$  and the 24-OH group of calcipotriol are shown as red and yellow dashed lines, respectively. (B) Model of VDR-ZK159222 in VDR-calcipotriol complex (blue). Superposition of calcipotriol in stick representation with carbon and oxygen atoms in gray and red, respectively, and of two conformers of ZK159222. One conformer (in cyan) with the cyclopropyl orientated as in the VDR-calcipotriol crystal structure presents a steric clash with H3. In the other conformer (in pink), the cyclopropyl is rotated and the last four carbon atoms lie between H3 and H12. The resulting steric hindrance is most likely responsible for the displacement of H12 and the resulting antagonist effect.

Like KH1060 (Figure 1), seocalcitol presents a longer side chain and additional methyl groups (C26a, C27a) compared to  $1\alpha,25(\text{OH})_2\text{D}_3$ . As seen in Figure 4B, because of the increased rigidity of the side chain of seocalcitol induced by the double bonds, the length between C17 and C25 is longer in VDR-seocalcitol (7.2 Å) compared to VDR-KH1060 (6.7 Å). As a consequence, the 25-OH group is shifted by 0.4 Å. Additional contacts of the methyl groups with H3, H11, and H12 observed in the two complexes are similar (Table 2). Like in VDR-KH1060,<sup>16</sup> where only the C26a group shows structural disorder, the weaker density of the electron density map at positions C26a and C27a of seocalcitol indicates a disorder of the two methyl groups in the crystals and their ability to adopt different conformations. Their higher *B* values (30–40) compared to *B* values of the rest of the ligand (between 10 and 20) reflect this mobility.

**Antagonism of ZK159222 and ZK168281.** Two different types of antagonist ligands have been identi-

**Table 2.** Protein/Ligand Aliphatic Side Chain Interactions Observed in the  $1\alpha,25(\text{OH})_2\text{D}_3$ , Calcipotriol, Seocalcitol, and KH1060 VDR LBD Complexes

residue	atom	$1\alpha,25(\text{OH})_2\text{D}_3$	calcipotriol	seocalcitol	KH1060
Leu227 (H3)	CD1	C26(3.5)	C26(3.5)	C26(3.5) C26a(3.2) C26a(3.8)	C26(3.4)
Ala231 (H3)	N CA CB		C27(4.0)	C26a(3.6) C27a(3.9)	C27a(3.7)
Val234 (H3)	CG1 CG2	C24(3.9)	C25(3.7)	C24(3.9)	C27(3.8) C27a(4.0)
Val300 (H6) His305 (6–7)	NE2	25-OH (2.7) C23(3.6) C25(3.7) C26(3.8)	25-OH(2.8) C23(3.6) C24(3.7)	25-OH(2.9) C23(4.0) C24(4.0) C24a(3.4) C25(3.7)	25-OH (2.9) C24(3.4) C26(3.8)
	CD2	C23(3.9)	C23(3.9)	C23(4.0) C24a(3.9)	C23(3.9) C24(3.6)
Leu309 (H7) His397 (H11)	CD2 CE1 NE2	C21(3.8) 25-OH(2.8) C24(3.7) C25(3.7)	C21(3.5) 25-OH(2.7) C24(3.5)	C21(3.6) C27a(3.6) 25-OH(2.9) C25(3.9)	C21(3.8) C27(4.1) 25-OH(2.6)
Leu414 (H12) Val418 (H12) Phe422 (H12)	CD2 CG1 CD1	C27(3.8)		C26a(3.6) C27(4.0) C27a(3.5)	C27a(3.9)

fied for VDR. The first type<sup>17</sup> of ligand exhibits a 25-carboxylic ester moiety in the flexible chain, and the second type<sup>20</sup> exhibits a 23,26 lactone ring. The first group of molecules shares the calcipotriol skeleton but contains an extension at the 25-position (Figure 1). Depending on the length and the structure of this extension, these ligands act either as a partial agonist (ZK159222, Schering AG) or as a full antagonist (ZK168281, Schering AG). Docking the two Schering compounds in the binding pocket by anchoring the 24-hydroxyl group reveals that the chain, extending from the position 25 of these ligands, clashes with helix H3 (Leu230, Val234) as seen in Figure 3B. To avoid this, a rotation around the bond between C24 and C25 of the ligand (from  $-67^\circ$  in calcipotriol to  $-154^\circ$  in the ZK compounds) keeps the cyclopropyl and the carboxyl moiety of ZK159222 in the ligand binding pocket, close to H3 but further away from Phe422. In this orientation, the last four carbon atoms extend toward helices H3 and H12. The aliphatic chain, if too short, can snuggle in small cavities. By extension of this carbon chain, steric contacts are observed with Ala231 (H3) and Val418 (H12), suggesting that most likely the activation helix will not be optimally positioned. With ZK159222, the displacement of H12 still allows an interaction with coactivators (20% of  $1\alpha,25(\text{OH})_2\text{D}_3$ ).<sup>21</sup> In contrast, ZK168281 exhibits a much larger and rigid chain because of the shifted carboxyl group and the introduction of a double bond between the cyclopropyl and the carboxyl group. This bulky chain more severely clashes with H12, which would explain the 5% agonist activity.<sup>21</sup>

## Conclusion

These two new crystal structures of VDR LBD complexes confirm that VDR can accommodate a large number of ligands with a modified side chain. This is consistent with the observation made on the structures of VDR superagonists with a common conformation of VDR bound to agonists or superagonists ligands. On the basis of the VDR-calcipotriol structure, new antagonists with high affinity can be designed. These antagonist

ligands with increased length of the side chain displaced the helix H12 function, analogous to the classical antagonists of ER.<sup>22</sup>

## Experimental Section

**Abbreviations.** NR, nuclear receptor; VDR, vitamin D nuclear receptor; LBD, ligand binding domain;  $1\alpha,25(\text{OH})_2\text{D}_3$ ,  $1\alpha,25$ -dihydroxyvitamin D<sub>3</sub>.

**Crystallography. (a) Expression, Purification, and Crystallization.** The LBD of the human VDR (residues 118–427  $\Delta$ 165–215) was cloned in pET28b expression vector to obtain an N-terminal hexahistidine-tagged fusion protein and was overproduced in *E. Coli* BL21 (DE3) strain. Cells were grown in LB medium and subsequently induced for 6 h at 20 °C with 1 mM isopropyl thio- $\beta$ -D-galactoside. The purification included a metal affinity chromatography step on a cobalt-chelating resin. After tag removal by thrombin digestion, the protein was further purified by gel filtration. The final protein buffer was 10 mM Tris, pH 7.5, 100 mM NaCl, and 5 mM dithiothreitol. The protein was concentrated to 10 mg/mL and incubated in the presence of a 5-fold excess of ligand. Purity and homogeneity were assessed by SDS and native PAGE and denaturant and native electrospray ionization mass spectrometry. Crystals of the different complexes were obtained at 4 °C by vapor diffusion in hanging drops. Reservoir solutions contained 0.1 M Mes, pH 6.0, and 1.4 M ammonium sulfate and appeared after 4 days.

**(b) X-ray Crystallography Data Collection and Processing.** Crystals were mounted in a capillary. One single native data set was collected for each complex at 4 °C at the beamlines BM14 and BM30 of the European Synchrotron Radiation Facility (Grenoble, France). Data were processed using the program HKL2000.<sup>24</sup>

**(c) Structure Determination and Refinement.** Initial phase estimates were obtained by omitting the  $1\alpha,25(\text{OH})_2\text{D}_3$  from the structure of the VDR- $1\alpha,25(\text{OH})_2\text{D}_3$  complex previously solved. After a rigid body refinement with CNS,<sup>25</sup> the refinement proceeded with iterative cycles of least-squares minimization and manual model building using the program O.<sup>26</sup> The ligand molecules were only included at the last stage of the refinement. Anisotropic scaling and a bulk solvent correction were used. Individual B atomic factors were refined anisotropically. Solvent molecules were then placed according to unassigned peaks in the difference Fourier maps. All of the refined models showed unambiguous chirality for the ligands and no Ramachandran plot outliers according to procheck. For

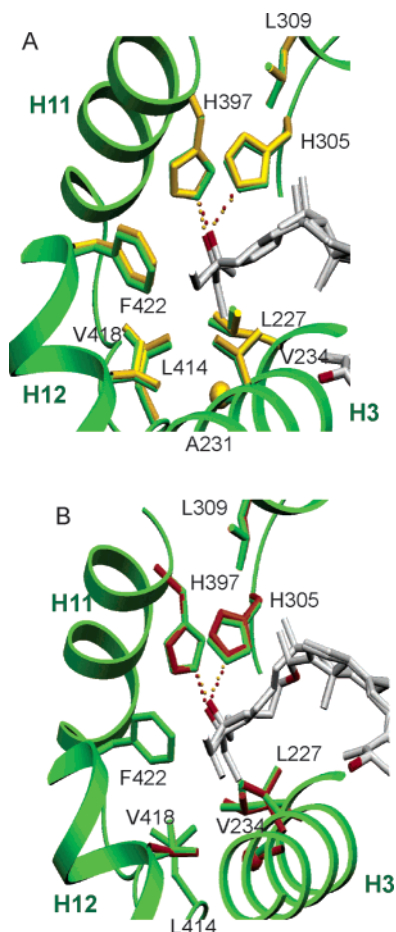


**Figure 4.** VDR-seocalcitol. (A) Superposition of the VDR-seocalcitol (green) and VDR- $1\alpha,25(\text{OH})_2\text{D}_3$  (yellow) complexes. The view is restricted to the region of the protein (H3, H6, H11, and H12) contacting the aliphatic side chain. Only residues closer than 4.0 Å are shown. The ligands  $1\alpha,25(\text{OH})_2\text{D}_3$  and seocalcitol are shown in stick representation with carbon and oxygen atoms gray and red, respectively. The hydrogen bonds formed by the 25-OH groups of  $1\alpha,25(\text{OH})_2\text{D}_3$  and seocalcitol are shown as red and yellow dashed lines, respectively. As a consequence of its longer side chain, the D ring of seocalcitol shifts by 0.4 Å, which results in a displacement of 0.7 Å for C21 compared to  $1\alpha,25(\text{OH})_2\text{D}_3$ . (B) Superposition of the VDR-seocalcitol (green) and VDR-KH1060 (orange) complexes in the same region. The same interactions are observed in the two complexes. Only residues closer than 4.0 Å are shown. The ligands seocalcitol and KH1060 are shown in stick representation with carbon and oxygen atoms in gray and red, respectively. The hydrogen bonds formed by the 25-OH groups of the ligands are shown as red and yellow dashed lines, respectively. Because of the increased rigidity of the side chain of seocalcitol induced by the double bonds, the length between C17 and C25 is longer in VDR-seocalcitol than in VDR-KH1060.

the VDR-seocalcitol complex, the weaker density of the electron density map at positions C26a and C27a of the ligand indicates a disorder of these methyl groups and their ability to adopt different conformations. The volumes of the ligand-binding pockets and ligands were calculated as previously reported.<sup>15</sup> Modeling experiments were performed as described.<sup>27</sup>

**Protein Data Bank Accession Number.** The accession numbers for the coordinates of the structures VDR-calcipotriol and VDR-seocalcitol reported in this article are 1S19 and 1S0Z, respectively.

**Acknowledgment.** We are grateful to A. Steinmeyer (Schering AG) for a generous gift of calcipotriol

and seocalcitol ligands. We thank A. Mitschler and the staff of the beamlines BM30 and BM14 at the European Synchrotron Radiation Facility (ESRF, Grenoble, France) for technical assistance during data collection. This work was supported by grants from CNRS, INSERM, Hôpital Universitaire de Strasbourg, and Ministère de la Recherche et de la Technologie. This work benefits from the technical platform of structural genomics supported by the Genopole and SPINE programs.

## References

- (1) Bouillon, R.; Okamura, W. H.; Norman, A. W. Structure–function relationships in the vitamin D endocrine system. *Endocr. Rev.* **1995**, *16*, 200–257.
- (2) Beckman, M. J.; Deluca, H. F. Modern view of vitamin D<sub>3</sub> and its medicinal uses. *Prog. Med. Chem.* **1998**, *35*, 1–56.
- (3) Stein, M. S.; Wark, J. D. An update on the therapeutic potential of vitamin D analogues. *Expert Opin. Invest. Drugs* **2003**, *12* (5), 825–840.
- (4) Calverley, M. J. Synthesis of MC903, a biologically active vitamin D metabolite analogue. *Tetrahedron* **1987**, *43*, 4609–4619.
- (5) Kraghalla, K.; Iversen, L. Calcipotriol. A new topical antipsoriatic. *Dermatol. Clin.* **1993**, *11*, 137–141.
- (6) Mizwicki, M. T.; Norman, A. W. Two key proteins of the vitamin D endocrine system come into crystal clear focus: comparison of the X-ray structures of the nuclear receptor for  $1\alpha,25(\text{OH})_2$  vitamin D<sub>3</sub>, the plasma vitamin D binding protein, and their ligands. *J. Bone Miner. Res.* **2003**, *18* (5), 795–806.
- (7) Kissmeyer, A. M.; Binderup, L. Calcipotriol (MC 903): pharmacokinetics in rats and biological activities of metabolites. A comparative study with  $1,25(\text{OH})_2\text{D}_3$ . *Biochem. Pharmacol.* **1991**, *41* (11), 1601–1606.
- (8) Hansen, C. M.; Hamberg, K. J.; Binderup, E.; Binderup, L. Seocalcitol (EB 1089): A vitamin D analogue of anti-cancer potential. Background, design, synthesis, pre-clinical and clinical evaluation. *Curr. Pharm. Des.* **2000**, *6* (7), 803–828.
- (9) Colston, K. W.; Mackay, A. G.; James, S. Y.; Binderup, L.; Chander, S.; Coombes, R. C. EB1089: a new vitamin D analogue that inhibits the growth of breast cancer cells *in vivo* and *in vitro*. *Biochem. Pharmacol.* **1992**, *44* (12), 2273–2280.
- (10) Evans, T. R.; Colston, K. W.; Lofts, F. J.; Cunningham, D.; Anthony, D. A.; Gogas, H.; de Bono, J. S.; Hamberg, K. J.; Skov, T.; Mansi, J. L. A phase II trial of the vitamin D analogue Seocalcitol (EB1089) in patients with inoperable pancreatic cancer. *Br. J. Cancer* **2002**, *86* (5), 680–685.
- (11) Mangelsdorf, D. J.; Thummel, C.; Beato, M.; Herrlich, P.; Schutz, G.; Umesono, K.; Blumberg, B.; Kastner, P.; Mark, M.; Chambon, P.; et al. The nuclear receptor superfamily: the second decade. *Cell* **1995**, *83*, 835–839.
- (12) Kalkhoven, E.; Valentine, J. E.; Heery, D. M.; Parker, M. G. Isoforms of steroid receptor co-activator 1 differ in their ability to potentiate transcription by the oestrogen receptor. *EMBO J.* **1998**, *17*, 232–243.
- (13) Kamei, Y.; Xu, L.; Heinzel, T.; Torchia, J.; Kurokawa, R.; Glass, C. K.; Lin, S. C.; Heyman, R. A.; Rose, D. W.; Glass, C. K.; Rosenfeld, M. G. A CBP integrator complex mediates transcriptional activation and AP-1 inhibition by nuclear receptors. *Cell* **1996**, *85*, 403–414.
- (14) Rachez, C.; Lemon, B. D.; Suldan, Z.; Bromleigh, V.; Gamble, M.; Naar, A. M.; Erdjument-Bromage, H.; Tempst, P.; Freedman, L. P. Ligand-dependent transcription activation by nuclear receptors requires the DRIP complex. *Nature* **1999**, *398*, 824–828.
- (15) Rochel, N.; Wurtz, J. M.; Mitschler, A.; Klaholz, B.; Moras, D. The crystal structure of the nuclear receptor for vitamin D bound to its natural ligand. *Mol. Cell* **2000**, *5*, 173–179.
- (16) Tocchini-Valentini, G.; Rochel, N.; Wurtz, J. M.; Mitschler, A.; Moras, D. Crystal structures of the vitamin D receptor complexed to superagonist 20-epi ligands. *Proc. Natl. Acad. Sci. U.S.A.* **2001**, *98*, 5491–5496.
- (17) Wiesinger, H.; Ulrich, M.; Fährnrich, M.; Haberey, M.; Neef, G.; Schwarz, K.; Kirsch, G.; Langer, G.; Thieroff-Ekerdt, R.; Steinmeyer, A. A novel vitamin D receptor partial agonist. *J. Invest. Dermatol.* **1998**, *110*, 532.
- (18) Vaisanen, S.; Ryhanen, S.; Saarela, J. T.; Perakyla, M.; Andersin, T.; Maenpaa, P. H. Structurally and functionally important amino acids of the agonistic conformation of the human vitamin D receptor. *Mol. Pharmacol.* **2002**, *62*, 788–794.
- (19) Rochel, N.; Tocchini-Valentini, G.; Egea, P. F.; Juntunen, K.; Garnier, J. M.; Vihko, P.; Moras, D. Functional and structural characterization of the insertion region in the ligand binding

- domain of the vitamin D nuclear receptor. *Eur. J. Biochem.* **2001**, *268*, 971–979.
- (20) Ishizuka, S.; Miura, D.; Ozono, K.; Chokki, M.; Mimura, H.; Norman, A. W. Antagonistic Actions in Vivo of (23S)-25-Dehydro-1 $\alpha$ -Hydroxyvitamin D(3)-26,23-Lactone on Calcium Metabolism Induced by 1 $\alpha$ ,25-Dihydroxyvitamin D(3). *Endocrinology* **2001**, *142* (1), 59–67.
- (21) Herdick, M.; Steinmeyer, A.; Carlberg, C. Carboxylic ester antagonists of 1 $\alpha$ ,25-dihydroxyvitamin D(3) show cell-specific actions. *Chem. Biol.* **2000**, *7* (11), 885–894.
- (22) Pike, A. C.; Brzozowski, A. M.; Walton, J.; Hubbard, R. E.; Thorsell, A. G.; Li, Y. L.; Gustafsson, J. A.; Carlquist, M. Structural insights into the mode of action of a pure antiestrogen. *Structure* **2001**, *9* (2), 145–153.
- (23) Bury, Y.; Steinmeyer, A.; Carlberg, C. Structure activity relationship of carboxylic ester antagonists of the vitamin D(3) receptor. *Mol. Pharmacol.* **2000**, *58*, 1067–1074.
- (24) Otwinowski, Z.; Minor, W. Processing X-ray data collected in oscillation mode. *Methods Enzymol.* **1997**, *276*, 307–326.
- (25) Brunger, A. T.; Adams, P. D.; Clore, G. M.; DeLano, W. L.; Gros, P.; Grosse-Kunstleve, R. W.; Jiang, J. S.; Kuszewski, J.; Nilges, M.; Pannu, N. S.; et al. Crystallography & NMR system: A new software suite for macromolecular structure determination. *Acta Crystallogr., Sect. D: Biol. Crystallogr.* **1998**, *54*, 905–921.
- (26) Jones, T. A.; Zou, J. Y.; Cowan, S. W.; Kjeldgaard, M. Improved methods for building protein models in electron density maps and the location of errors in these models. *Acta Crystallogr. A* **1991**, *47*, 110–119.
- (27) Wurtz, J. M.; Guillot, B.; Fagart, J.; Moras, D.; Tietjen, K.; Schindler, M. A new model for 20-hydroxycyclopropane and dibenzoylhydrazine binding: a homology modeling and docking approach. *Protein Sci.* **2000**, *9*, 1073–1084.

JM0310582